An optimisation design of the combined np-CUSUM scheme for attributes

Salah Haridy* and Zhang Wu

School of Mechanical and Aerospace Engineering,
Nanyang Technological University,
639798, Singapore
E-mail: salah@pmail.ntu.edu.sg
E-mail: mzwu@ntu.edu.sg
*Corresponding author

Fong-Jung Yu

College of Engineering,
Da-Yeh University,
Chang Hua, 51591, Taiwan
E-mail: fischer@mail.dyu.edu.tw

Mohammad Shamsuzzaman

College of Engineering,
University of Sharjah,
Sharjah, 27272, UAE
E-mail: mshamsuzzaman@sharjah.ac.ae

Abstract: The np chart and the binomial cumulative sum (CUSUM) chart are attribute charts that monitor the fraction non-conforming *p*. While the np chart is effective for detecting large process shifts in *p*, the CUSUM chart is more powerful for detecting small and moderate *p* shifts. This article presents an optimisation algorithm for the design of the combined np chart and CUSUM chart (the np-CUSUM scheme). This design algorithm not only optimises the charting parameters of the np chart element and CUSUM chart element, but also optimises the allocation of detection power between the two chart elements, so that the best overall performance can be achieved. The np-CUSUM scheme has the salient features of the np chart and the CUSUM chart. The performance of the np-CUSUM scheme is compared with that of other charts in a systematic and quantitative manner. The results show that the optimal np-CUSUM scheme always outperforms, or at least performs equally as, the individual np chart, CUSUM chart and binomial exponentially weighted moving average (EWMA) chart by 222%, 5% and 11%, respectively, in terms of the average number of defectives (*AND*), under different conditions.
[Received 30 November 2010; Revised 21 February 2011; Accepted 3 May 2011]

Keywords: attribute chart; np chart; cumulative sum chart; np-CUSUM scheme; optimisation design; quality control.

Copyright © 2013 Inderscience Enterprises Ltd.

Reference to this paper should be made as follows: Haridy, S., Wu, Z., Yu, F-J. and Shamsuzzaman, M. (2013) 'An optimisation design of the combined np-CUSUM scheme for attributes', *European J. Industrial Engineering*, Vol. 7, No. 1, pp.16–37.

Biographical notes: Salah Haridy is a PhD student in the School of Mechanical and Aerospace Engineering at Nanyang Technological University, Singapore. He gained his MSc in 2008 and BSc in 2004 in Mechanical Engineering and Technology from Benha University, Egypt. His current research work focuses on the statistical process control, the developments of algorithms in quality control, process capability and design of experiments.

Zhang Wu is an Associate Professor in the School of Mechanical and Aerospace Engineering at Nanyang Technological University, Singapore. He gained his PhD in 1988 and MEng in 1984 from McMaster University, Canada, and gained his BEng in 1982 from Huazhong University of Science and Technology, China. His current research interests include the developments of algorithms in quality control, reliability, non-linear optimisation and geometrical tolerance. He is a senior member of the American Society for Quality.

Fong-Jung Yu is a Professor at the Department of Industrial Engineering and Technology Management, Da-Yeh University, Taiwan. He received his PhD in 2002 and Master in 1992 from Yuan Ze University, Taiwan, and gained his Bachelor degree in 1977 from Chung-Yuan College of Science and Engineering. His research focuses on SPC, TQM, Six Sigma and quality related fields. He worked for a fighter programme at logistic engineering department of Chung Shan Institute of Science and Technology for over 12 years before he came to Da-Yeh University and also worked at the industrial engineering related field of several factories from June 1977 to October 1984. He also gained the individual award of quality award from Chinese Society for quality in 2010.

Mohammad Shamsuzzaman is an Assistant Professor in the Department of Industrial Engineering and Management at Sharjah University, UAE. He received his MEng and PhD in Industrial Engineering from Asian Institute of Technology, Thailand and Nanyang Technological University, Singapore in 2000 and 2005, respectively. His research interests fall into the following domains: quality control, fuzzy logic, and multicriteria decision-making.

1 Introduction

Quality control (QC) is nowadays one of the most important activities in industries and service sectors (Chan et al., 2009; Parveen and Rao, 2009; Raj and Attri, 2010). The quality of a process can be achieved by statistical process control (SPC). The control chart developed in SPC is an effective online monitoring technique widely used in manufacturing industry and other sectors. Many new charts and SPC techniques have been proposed in recent years (Wu et al., 2006; Garcia-Diaz, 2007).

The np control chart is a simple attribute chart used to check the number d of non-conforming units found in a sample. The widespread applications of the np chart and other attribute charts are attributable to several factors, such as the simplicity of handling attribute quality characteristics, the capability of checking multiple quality requirements, the ease to communicate between people at different levels, and the prevalence of count data in many non-manufacturing sectors. The np chart is equivalent to the p chart when the sample size is constant. The fraction non-conforming p is defined as the ratio between the number of non-conforming units in a population and the total number of units in that population. When running an np chart, the process is considered to be in control if d satisfies $LCL \leq d \leq UCL$. Here, LCL and UCL are the lower and upper control limits of the np chart. However, if $d < LCL$, a downward p shift is signalled, and if $d > UCL$, then an upward p shift is signalled.

Unlike the np chart that only uses the information about d in the last sample, the binomial cumulative sum chart (CUSUM chart in short) incorporates all the information in the sequence of observed values of d (Lucas, 1985a). While the CUSUM chart is more sensitive to small and moderate shifts in fraction non-conforming p, it is less effective than the np chart for detecting large p shifts. The reason is that the CUSUM chart does not make a decision merely based on the data in the latest sample and is therefore unable to respond promptly to a sudden and large p shift. A statistic C_t is updated and plotted for the t^{th} sample in a CUSUM chart for detecting upward p shifts.

$$
\begin{aligned}
C_0 &= 0 \\
C_t &= \max\left(0, C_{t-1} + \left(d_t - d_0\right) - k_0\right) \\
&= \max\left(0, C_{t-1} + d_t - \left(d_0 + k_0\right)\right)
\end{aligned} \tag{1}
$$

where d_t is the number of non-conforming units found in the t^{th} sample, d_0 is the in-control value of d equal to (np_0), and k_0 is the initial reference parameter. In equation (1), the constant term ($d_0 + k_0$) can be replaced by a single reference parameter k so that equation (1) can be simplified as follows:

$$
\begin{aligned}
C_0 &= 0 \\
C_t &= \max\left(0, C_{t-1} + d_t - k\right)
\end{aligned} \tag{2}
$$

When an increasing p shift occurs, C_t tends to become larger and larger. Sooner or later, a sample point will exceed the control limit H of the CUSUM chart, and thereby an out-of-control signal is produced.

Another effective tool for detecting small and moderate shifts in fraction non-conforming p is the binomial exponentially weighted moving average (EWMA) chart (Roberts, 1959). This chart also uses cumulative information from all samples up to the last one and has quite similar operating characteristics as the CUSUM chart (Reynolds and Stoumbos, 2004a). A statistic E_t is updated and plotted for the t^{th} sample in an EWMA chart for detecting upward p shifts.

$$
\begin{aligned}
E_0 &= 0 \\
E_t &= \max\left(0, \lambda\left(d_t - d_0\right) + (1-\lambda)E_{t-1}\right)
\end{aligned} \tag{3}
$$

The parameters of an EWMA chart include the smoothing parameter λ ($0 < \lambda \leq 1$) and the control limit W. This chart produces an out-of-control signal when E_t becomes larger than W.

The CUSUM and EWMA charts have been increasingly recognised across industries for SPC applications (Zhao et al., 2005; Shu et al., 2008). It is mainly attributed to the fact that online measurement and distributed computing systems become a norm in today's SPC applications (Woodall and Montgomery, 1999). Woodall (1984) described a Markov chain representation of the binomial CUSUM chart. Hawkins (1992) proposed a general algorithm for evaluating the average run length (*ARL*) of this chart. White and Keats (1996) developed a computer programme to calculate the *ARL* for the Poisson CUSUM scheme. Brook and Evans (1972) proposed a Markov chain approach to calculate the *ARL* of the binomial EWMA control chart. Lucas (1985b) detailed the design and implementation for the binomial CUSUM chart. Gan (1993) further developed an optimisation algorithm to minimise the average time to signal (*ATS*) at a particular p shift value. Epprecht et al. (2010) proposed an optimal design for the attribute EWMA chart with variable sampling interval. Lucas (1989) studied in particular the performance of the binomial CUSUM chart when the defect level is very low and Bourke (2001) investigated the operating characteristics of this chart under 100% inspection. Radaelli (1994) examined the Poisson approximation to the binomial CUSUM chart. Wu and Tian (2005) proposed a CUSUM chart based on the weighted loss function. Wu et al. (2008a) studied a unique feature of the binomial CUSUM chart with an exponential w depending on the size of process shift. Some researchers compared the performance of the binomial CUSUM chart with other charts such as the c chart (White et al., 1997) and the Bernoulli CUSUM chart (Reynolds and Stoumbos, 2000).

Lucas (1982) proposed a combined scheme of an $\bar{X}$ (or X) chart and a CUSUM chart. In his scheme, the CUSUM feature will quickly detect small and moderate mean shifts while the addition of the $\bar{X}$ chart increases the speed of detecting large mean shifts. Lucas (1982) also commented that the combined $\bar{X}$ and CUSUM scheme is almost as easy to use as a single CUSUM chart. Wu et al. (2008b) proposed an algorithm for the optimisation design of Lucas's combined $\bar{X}$ and CUSUM scheme. Their algorithm effectively improves the overall performance of the combined $\bar{X}$ and CUSUM scheme over the entire mean shift range. Yashchin (1985) considered combined CUSUM-Shewhart schemes for detecting one- and two-sided process shifts. Yashchin (1985) and Abel (1990) addressed the use of the combined CUSUM-Shewhart control schemes for count data that follow a Poisson distribution.

Morais and Pacheco (2006) discussed the upper one-sided combined CUSUM-Shewhart scheme for binomial data (referred as the *M-P np-CUSUM* chart in this article). However, they did not develop a systematic procedure to design the combined scheme. An np chart and a CUSUM chart are simply put together without optimising the charting parameters or allocating the detection power between the np chart element and the CUSUM chart element. Moreover, the design aims at minimising the out-of-control *ATS* at a specified p shift. However, it is usually difficult to predict the magnitudes or sizes of process shifts in most SPC applications (Reynolds and Stoumbos, 2004b). A control chart should be designed to produce a small out-of-control *ATS* for p shifts of different sizes, or have an excellent overall performance across the entire shift range of interest. Even though the performance of the M-P np-CUSUM chart has been compared with that of some other charts, a clear conclusion has not been reached. Morais and Pacheco (2006) mentioned that the M-P np-CUSUM scheme is better than np chart for detecting smaller p shifts and outperforms the single CUSUM chart for detecting larger p shifts, but they did not infer which chart is better from an overall viewpoint and to what degree. They concluded that the combined np-CUSUM scheme may not be necessarily better than the individual charts from an overall viewpoint. Another problem pertaining to the M-P np-CUSUM chart is that it often fails to satisfy the requirement on the false alarm rate.

This article proposes an optimisation design of the combined scheme comprising an np chart and a CUSUM chart, called the *np-CUSUM scheme*. This design algorithm not only optimises the charting parameters of each of the np chart element and the CUSUM chart element, but also optimises the allocation of detection power between the two chart elements. The objective is to achieve the best overall performance. The performance of the np-CUSUM scheme will be compared with that of other charts in a systematic and analytical manner. The results show that this optimal np-CUSUM scheme is quite effective for detecting both small and large p shifts, and its overall performance is always better than, or at least as good as, that of the individual np chart, CUSUM chart and EWMA chart. The high effectiveness of the np-CUSUM scheme is attributable to the optimisation design of the combined control scheme as well as the concurrent use of the information regarding the last sample and the information from the series of the previous sample points.

The operating characteristic of a control chart is usually measured by the ATS. While a small out-of-control ATS means prompt signalling of process shifts, a large in-control ATS_0 indicates low false alarm rate. In this article, the out-of-control ATS is calculated using the steady-state mode which allows the p shift to take place at any time within a sampling interval.

In this article, the sampling interval h is taken as the time unit (i.e., $h = 1$), therefore, the ARL is equal to ATS. The sampling interval h is determined by using the rational subgroup concept. A rational subgroup is a group of units or a sample of size n. The n units to be inspected in a sample are produced at the same time (or as closely together as possible) and under a condition that only random effects are responsible for the observed variation (Nelson, 1988). Subgroups must be representative of process operation.

In this article, it is assumed that the random number d (the number of non-conforming units found in a sample) follows a binomial distribution with known in-control fraction non-conforming p_0. When a process shift occurs, the fraction non-conforming p will change to

$$p = \delta p_0, \tag{4}$$

where ($\delta \geq 1$) is the shift in terms of p_0. $\delta = 1$ means that the process is in control.

Since the control charts for attributes are most often used to detect an increase in fraction non-conforming or deterioration in quality (Lucas, 1985a; Reynolds and Stoumbos, 1999), the focus of this research is to detect increasing p shifts.

The remainder of the article proceeds as follows. Firstly, the implementation and design of the np-CUSUM scheme are presented. Then, a comparison of five control charts including the M-P np-CUSUM chart and np-CUSUM scheme is presented. Subsequently, a case study is illustrated. The conclusions and discussions are drawn in the last section.

2 Implementation and design of the np-CUSUM scheme

An np-CUSUM scheme consists of a CUSUM chart element and an np chart element. It has three parameters: the control limit H and reference parameter k for the CUSUM element and the upper limit *UCL* for the np element. An np-CUSUM scheme is implemented as follows:

1 Initialise the statistic C_0 in equation (2) as zero.

2 Take a sample of *n* units at the end of each sampling interval *h* and count the number d_t of non-conforming units in this sample.

3 Update C_t as follows [referring to equation (2)]

$$C_t = \max\left(0,\ C_{t-1} + d_t - k\right) \tag{5}$$

4 If $C_t \le H$ and $d_t \le UCL$, the process is thought to be in control, and go back to step (2) for the next sample.

5 Otherwise (i.e., $C_t > H$ and/or $d_t > UCL$), an out-of-control signal is produced and the process is stopped immediately for further investigation.

These steps can also serve as the pseudo code for developing an operational programme for the computer-aided implementation. It is noted that ($d_t > UCL$) is the only addition for the implementation of an np-CUSUM scheme compared with the individual CUSUM chart. While the CUSUM chart produces an out-of-control signal only when ($C_t > H$), an np-CUSUM scheme signals when ($C_t > H$) and/or ($d_t > UCL$). Checking the condition of ($d_t > UCL$) only slightly increases the difficulty in implementation, but it significantly enhances the capability of the np-CUSUM scheme for detecting large *p* shifts.

To design an np-CUSUM scheme, the following four specifications need to be determined beforehand:

1 the allowable minimum value τ of in-control ATS_0

2 the in-control fraction non-conforming p_0

3 the maximum out-of-control value $p_{\max}$ of fraction non-conforming

4 the sample size *n*.

The value of τ is decided with regards to the tolerable false alarm rate. The value of p_0 is usually estimated from the data observed during the pilot runs in phase I test. The control charts used in phase I and phase II may not be the same. For example, in variable control charts, Montgomery (2009) suggested using an $\bar{X}$ chart in phase I to collect the data for the estimation of process parameters, and then designing a more advanced EWMA or CUSUM chart to monitor the same process in phase II. Likewise, an np chart could be used in phase I to estimate p_0 in order to construct the np-CUSUM scheme. Then, the np-CUSUM scheme is used in phase II to monitor the process shift in fraction non-conforming.

The maximum fraction non-conforming $p_{\max}$ is required for the calculation of the average number of defectives (*AND*) which will be discussed shortly. $p_{\max}$ may be chosen based on the knowledge about a process (e.g., the maximum possible *p* shift in a process) or taken as the shift range the users are interested. The sample size *n* is usually determined according to the available resources (such as manpower and instruments) and the requirements on detection effectiveness. A large sample size will increase the detection effectiveness of the np-CUSUM scheme and any other charts but make the inspection more costly. British Standard Institution Handbook 24 (1985) suggested determining n by:

$$n = \frac{r}{p_0} \tag{6}$$

where r is a constant between 1 and 3 when $p_0 \geq 0.03$ and should be made smaller along with the decrease of p_0.

It is usually difficult to predict the magnitudes or sizes of process shifts in most applications (Reynolds and Stoumbos, 2004b). Therefore, a control chart should produce a small out-of-control *ATS* for process shifts of different sizes, or have an excellent overall performance across the entire shift range of interest. The *AND* can be adopted to measure the overall performance of an attribute control chart. It is the average number of non-conforming units produced in different out-of-control cases over a process shift range of ($p_0 < p_i \leq p_{\max}$). If N is the number of units produced per time unit and $ATS(p_i)$ is the *ATS* value that corresponds to a particular out-of-control case in which the fraction non-conforming is $p_i(= i \times p_0)$, then the number of defectives produced during this particular out-of-control case is $N \times p_i \times ATS(p_i)$. If $(m - 1)$ different p_i values are taken into consideration (i.e., $p_i = i \times p_0$, $i = 2, 3, \ldots\ldots, m$), then the average number of non-conforming units for all out-of-control cases is *AND*, that is

$$AND = \frac{1}{m-1}\sum_{i=2}^{m}\left(N \cdot p_i \cdot ATS\left(p_i\right)\right) = \frac{N}{m-1}\sum_{i=2}^{m}\left(p_i \cdot ATS\left(p_i\right)\right) \tag{7}$$

Since N is a constant and has no effect on the performance comparison and the optimal solution, it can be omitted from equation (7). Then,

$$AND = \frac{1}{m-1}\sum_{i=2}^{m} p_i ATS\left(p_i\right). \tag{8}$$

The index *AND* directly relates the chart performance with the economic outcome. That is, a chart producing smaller *AND* will produce less number of defectives, on average, when out-of-control cases occur. Moreover, *AND* can be considered as a weighted average of *ATS* that uses p as the weight. It means that if *AND* is used as the objective function to be minimised, then the larger the p_i, the smaller the corresponding $ATS(p_i)$ will be resulted from the optimisation design. The out-of-control $ATS(p_i)$ of the np-CUSUM scheme is calculated by the formulae derived in the Appendix.

In this article, the design of the np-CUSUM scheme will be carried out based on the following optimisation model using *AND* as the objective function:

$$\text{Objective:} \quad \text{Minimise} \quad AND \tag{9}$$

$$\text{Constraint:} \quad ATS_0 \geq \tau, \tag{10}$$

$$\text{Design variables:} \quad UCL, k, H.$$

where *UCL* and k are treated as independent design variables. The control limit H is dependent on *UCL*, k and the specified τ. The objective of the optimisation design is to identify the optimal values of *UCL* and k that minimise *AND* over a shift range of

($p_0 < p \le p_{\max}$), and meanwhile H is adjusted so that $ATS_0 \ge \tau$. The optimisation design is implemented by a two-level search as outlined below:

1 Specify the parameters τ, p_0, $p_{\max}$ and n.

2 Initialise a variable $AND_{\min}$ as a very large number, say 10^7 ($AND_{\min}$ is used to store the minimum value of AND).

3 At the first or top level, search the optimal value of UCL by increasing it one by one with a starting value of UCL_{np}, where UCL_{np} is the upper control limit of an np chart that meets ($ATS_0 \ge \tau$). It is noted that the UCL of the np-CUSUM scheme cannot be smaller than UCL_{np}, otherwise the constraint of ($ATS_0 \ge \tau$) must be violated. The search at this top level will be terminated when AND cannot be further reduced.

4 At the second or low level, with the given value of UCL determined at the top level, search the optimal value of k. For a given set of values of (UCL, k)
   - determine the control limit H that satisfies the constraint of ($ATS_0 \ge \tau$)
   - when the values of all three charting parameters, UCL, k and H, are preliminarily determined, calculate the objective function AND by equation (8)
   - if the calculated AND is smaller than the current $AND_{\min}$, replace the latter by the former and the current values of UCL, k and H are stored as a temporary optimal solution.

5 At the end of the entire two-level search, the optimal np-CUSUM scheme that produces the minimum AND and satisfies the constraint ($ATS_0 \ge \tau$) is identified. The corresponding optimal values of UCL, k and H are also finalised.

In the optimisation design, adjusting UCL is to allocate the Type I error (or power) of the np-CUSUM scheme between the np chart element and the CUSUM chart element. If UCL is tightened, H must be relaxed for ($ATS_0 \ge \tau$). This will make the np-CUSUM scheme more sensitive to large p shifts. Similarly, if UCL is loosened, H can be tightened, and the np-CUSUM scheme will be more powerful for detecting small p shifts. Furthermore, the reference parameter k is optimised in order to make the np-CUSUM scheme most effective for signalling different p shifts across the entire range rather than to minimise the out-of-control ATS value just for a particular p shift.

The above search mechanism is quite reliable, because the number of the possible values of the integral UCL is limited and can be tested one by one, and the optimal value of the only remaining variable, k, can be easily determined by an exhaustive search. For the cases tested in this article, the optimisation design of an np-CUSUM scheme can be completed within a few minutes of CPU time in a personal computer.

3 Comparative studies

In this section, the detection effectiveness of four control charts (the np chart, the CUSUM chart, the EWMA chart and the combined np-CUSUM scheme) is studied and compared. The charts are studied only for detecting increases in fraction non-conforming.

The design of an np chart is to adjust the upper control limit UCL so that the resultant ATS_0 is no smaller than τ. The design of a CUSUM chart is to find the best combination of the reference parameter k and the control limit H so, that the chart produces the minimum *AND* [equation (8)] and meanwhile has an ATS_0 equal to or larger than τ. The design of a EWMA chart is similar to the design of a CUSUM chart except that the two charting parameters to be adjusted are the smoothing parameter λ and the control limit W.

The four charts are first studied under a general case as shown below:

$$\tau = 650,\ p_0 = 0.01,\ p_{\max} = 10p_0 = 0.1 \text{ and } n = 1/p_0 = 100 \tag{11}$$

The four charts are designed for this case and the results are shown below:

np chart: $UCL = 5$.

CUSUM chart: $k = 1.750,\ H = 4.630$.

EWMA chart: $\lambda = 0.230,\ W = 1.275$.

np-CUSUM scheme: $k = 1.500,\ H = 6.011,\ UCL = 5$.

The *ATS* values of the four charts are calculated within the process shift range from p_0 to $p_{\max}$, and the results are displayed in Table 1. The curves of the normalised *ATS* (i.e., $ATS/ATS_{np\text{-}CUSUM}$) of the four charts are illustrated in Figure 1. Figure 1(a) shows the full scale normalised *ATS* curves while Figure 1(b) zooms in the curves over a smaller scale of $ATS/ATS_{np\text{-}CUSUM}$. It is interesting to observe the followings from Table 1 and Figure 1:

1. Firstly, each of the four charts generates an ATS_0 value close to or larger than τ when the process is in control. This ensures that the requirement on the false alarm rate is satisfied. It is noted that, the ATS_0 values of the CUSUM chart, EWMA chart and np-CUSUM scheme are fairly close to τ (= 650) because these three charts have several parameters that can be adapted to fit the constraint ($ATS_0 \geq \tau$). As a result, the potential effectiveness of these three charts can be better utilised. On the contrary, the np chart with only one integral parameter (*UCL*) generates an in-control ATS_0 (= 1,871) much larger than τ and, thus, has lower effectiveness (Reynolds and Stoumbos, 1999). However, an attempt to tighten the *UCL* (i.e., reducing *UCL* from five to four) will make the resultant ATS_0 equal to 291 that seriously violates the constraint ($ATS_0 \geq \tau$). It reflects an intrinsic drawback of the np charts due to the discrete nature of the attribute quality characteristics.

2. As expected, the CUSUM chart and EWMA chart outperform the np chart for small p shifts to a significant degree (when $p \leq 6p_0$), but they are less sensitive than the latter to larger p shifts (when $p > 7p_0$).

3. The *ATS* values of the np-CUSUM scheme are often either equal or close to the minimum across the p shift range. The np-CUSUM scheme becomes more superior to both CUSUM and EWMA charts for large p shifts ($p > 5p_0$) because the former is able to respond quickly to the change of p in the last sample. When $p = 8p_0$, the *ATS* values of the CUSUM chart and EWMA chart are larger than that of the np-CUSUM scheme by 13% and 7%, respectively. On the other hand, the np-CUSUM scheme outperforms the np chart over the entire p shift range, especially when p is small. For example, when $p = 2p_0$, the np chart produces an *ATS* larger than that of the np-CUSUM scheme by 483%. Obviously, it is the combination of the np and CUSUM charts plus the optimisation design that makes the np-CUSUM scheme very effective from an overall viewpoint. The np-CUSUM scheme is less effective than the CUSUM chart and EWMA chart only in a small region of p shifts (when p is around $4p_0$).

Table 1 Comparison of four charts at $\tau = 650$, $p_0 = 0.01$, $p_{max} = 10p_0$, $n = 100$

$p(\times p_0)$	*ATS*			
	np chart	*CUSUM chart*	*EWMA chart*	*np-CUSUM chart*
1	1,870.7868	741.4627	635.1933	673.3411
2	64.0843	11.9108	11.8273	11.0009
3	11.8706	3.8571	3.7590	3.9261
4	4.2253	2.2453	2.1261	2.2850
5	2.1042	1.5659	1.4844	1.5068
6	1.2879	1.1899	1.1045	1.0907
7	0.9113	0.9490	0.8844	0.8441
8	0.7193	0.7863	0.7402	0.6947
9	0.6167	0.6763	0.6453	0.6075
10	0.5611	0.6016	0.5844	0.5575

Figure 1 Normalised *ATS* of the four control charts

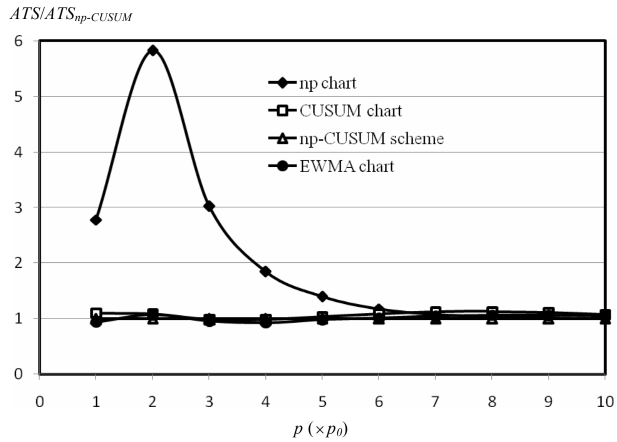

(a)

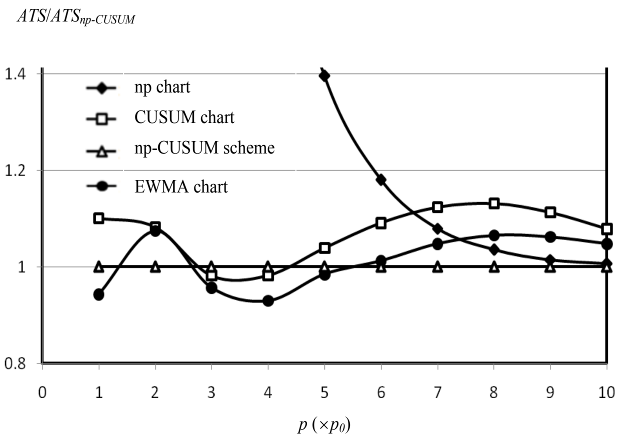

(b)

Table 2 Comparison of the four charts in a 2^k factorial design

Case	τ	p_0	$p_{max}(\times p_0)$	n	*Chart*	*k or λ*	*H or W*	*UCL*	*AND*	$AND/AND_{np-CUSUM}$
0	650	0.01	10	100	np	-	-	5	0.2469	2.8189
					CUSUM	1.750	4.630	-	0.0962	1.0982
					EWMA	0.230	1.275	-	0.0901	1.0285
					np-CUSUM	1.500	6.011	5	0.0876	1.0000
1	300	0.005	5	120	np			3	0.1425	1.7867
					CUSUM	0.950	4.333	-	0.0829	1.0397
					EWMA	0.410	1.402	-	0.0957	1.2008
					np-CUSUM	0.950	4.204	5	0.0797	1.0000
2	300	0.005	15	120	np	-	-	3	0.0671	1.2790
					CUSUM	0.950	4.236	-	0.0555	1.0575
					EWMA	0.365	1.294	-	0.0527	1.0038
					np-CUSUM	0.950	4.270	4	0.0525	1.0000
3	300	0.005	5	240	np	-	-	5	0.1128	2.4784
					CUSUM	2.150	3.725	-	0.0482	1.0583
					EWMA	0.275	1.404	-	0.0456	1.0022
					np-CUSUM	1.900	4.651	5	0.0455	1.0000
4	300	0.005	15	240	np	-	-	5	0.0527	1.5967
					CUSUM	2.150	3.703	-	0.0339	1.0270
					EWMA	0.365	1.741	-	0.0337	1.0212
					np-CUSUM	1.900	4.616	5	0.0330	1.0000
5	300	0.03	5	20	np	-	-	3	0.9394	2.0512
					CUSUM	0.950	4.173	-	0.4580	1.0000
					EWMA	0.365	1.260	-	0.5247	1.1456
					np–CUSUM	0.950	4.173	∞	0.4580	1.0000

Table 2 Comparison of the four charts in a 2^k factorial design (continued)

Case	τ	p_0	$p_{max}(\times p_0)$	*n*	*Chart*	*k or λ*	*H or W*	*UCL*	*AND*	$AND/AND_{np\text{-}CUSUM}$
6	300	0.03	15	20	np	-	-	3	0.4187	1.4208
					CUSUM	1.200	2.876	-	0.3022	1.0255
					EWMA	0.365	1.260	-	0.3025	1.0265
					np-CUSUM	0.950	5.349	3	0.2947	1.0000
7	300	0.03	5	40	np	-	-	5	0.7391	2.8538
					CUSUM	1.900	4.361	-	0.2670	1.0310
					EWMA	0.410	1.826	-	0.2828	1.0919
					np-CUSUM	1.900	4.472	5	0.2590	1.0000
8	300	0.03	15	40	np	-	-	5	0.3319	1.7190
					CUSUM	2.400	2.808	-	0.1990	1.0305
					EWMA	0.365	1.689	-	0.1968	1.0192
					np-CUSUM	1.900	4.400	5	0.1931	1.0000
9	900	0.005	5	120	np	-	-	4	0.5239	5.0414
					CUSUM	1.200	3.897	-	0.1121	1.0785
					EWMA	0.500	1.877	-	0.1552	1.4937
					np-CUSUM	0.950	5.424	5	0.1039	1.0000
10	900	0.005	15	120	np	-	-	4	0.1860	3.0341
					CUSUM	1.200	3.860	-	0.0663	1.0814
					EWMA	0.455	1.765	-	0.0726	1.1843
					np-CUSUM	0.950	5.646	4	0.0613	1.0000
11	900	0.005	5	240	np	-	-	6	0.3074	5.4161
					CUSUM	1.900	5.680	-	0.0581	1.0237
					EWMA	0.320	1.825	-	0.0635	1.1180
					np-CUSUM	1.900	5.791	6	0.0568	1.0000

Table 2 Comparison of the four charts in a 2^k factorial design (continued)

Case	τ	p_0	$p_{max}(\times p0)$	*n*	*Chart*	*k or* λ	*H or W*	*UCL*	*AND*	$AND/AND_{np-CUSUM}$
12	900	0.005	15	240	np	-	-	6	0.1101	2.9344
					CUSUM	1.900	5.697	-	0.0391	1.0419
					EWMA	0.185	1.247	-	0.0386	1.0293
					np-CUSUM	1.900	5.774	6	0.0375	1.0000
13	900	0.03	5	20	np	-	-	4	3.9678	6.5125
					CUSUM	1.200	3.897	-	0.6792	1.1148
					EWMA	0.410	1.584	-	0.8275	1.3581
					np–CUSUM	0.950	5.401	4	0.6093	1.0000
14	900	0.03	15	20	np	-	-	4	1.3414	3.8247
					CUSUM	1.200	3.806	-	0.3887	1.1083
					EWMA	0.365	1.462	-	0.3928	1.1200
					np-CUSUM	0.950	5.408	4	0.3507	1.0000
15	900	0.03	5	40	np	-	-	6	2.2024	6.4838
					CUSUM	1.900	5.512	-	0.3454	1.0168
					EWMA	0.185	1.224	-	0.3401	1.0012
					np-CUSUM	1.900	5.512	7	0.3397	1.0000
16	900	0.03	15	40	np	-	-	6	0.7595	3.4498
					CUSUM	2.150	4.700	-	0.2252	1.0230
					EWMA	0.275	1.598	-	0.2266	1.0291
					np-CUSUM	1.900	5.566	6	0.2202	1.0000

The *AND* values [equation (8)], as well as the ratio of ($AND/AND_{np\text{-}CUSUM}$), of the four charts are enumerated in case 0 in Table 2. The values of ($AND/AND_{np\text{-}CUSUM}$) indicate that, for this case (where $\tau = 650$, $p_0 = 0.01$, $p_{max} = 10p_0$ and $n = 100$), the np-CUSUM scheme reduces the *AND* by 181.89%, 9.82% and 2.85% compared with the np chart, CUSUM chart and EWMA chart, respectively, over the range of p shifts.

Next, the four charts are further studied under more different conditions through a 2^4 factorial experiment in which the four specifications (τ, p_0, p_{max} and n) are used as the input factors and each of them varies at two levels as shown below:

$$
\begin{array}{lll}
\tau: & 300, & 900 \\
p_0: & 0.005, & 0.03 \\
p_{\max}: & 5p_0, & 15p_0 \\
n: & 0.6/p_0 & 1.2/p_0.
\end{array}
$$

The levels are determined with reference to those commonly used by many authors (Gan, 1993; Wu et al., 2008a). It is noted that p_{max} and n are expressed in terms of p_0.

This 2^k experiment results in 16 different cases or combinations of τ, p_0, p_{max} and n as shown in Table 2 (in cases 1 to 16). For each case, the four control charts are designed and each of them produces an ATS_0 no smaller than τ. In all these 16 cases, the relative detection effectiveness of the charts is similar to that revealed in Table 1. Namely, the np-CUSUM scheme is always more effective than the other three charts in terms of *AND*, with only one exception in case 5 where the np-CUSUM scheme and CUSUM chart are identical and equally effective.

The overall performance, as reflected by *AND*, is summarised in Table 2 for the 16 cases. Also, the charting parameters are listed in Table 2. The values of $AND_{np}/AND_{np\text{-}CUSUM}$, $AND_{CUSUM}/AND_{np\text{-}CUSUM}$ and $AND_{EWMA}/AND_{np\text{-}CUSUM}$ are always no smaller than one. The np-CUSUM scheme always outperforms the np chart to a significant degree, especially when τ is large and/or p_{max} is small. The ratio of $AND_{np}/AND_{np\text{-}CUSUM}$ has its maximum value of 6.512 in case 13. Similarly, the np-CUSUM scheme is often considerably more effective than the CUSUM chart and EWMA chart, especially when τ is large and/or n is small. For example, in case 13, the ratios of $AND_{CUSUM}/AND_{np\text{-}CUSUM}$ and $AND_{EWMA}/AND_{np\text{-}CUSUM}$ are equal to 1.115 and 1.368, respectively.

Finally, a grand average $\overline{\dfrac{AND}{AND_{np\text{-}CUSUM}}}$ is calculated for each chart. It indicates the average of the $AND/AND_{np\text{-}CUSUM}$ values encompassing all the 16 cases in Table 2. The results are

$$\overline{\frac{AND_{np}}{AND_{np\text{-}CUSUM}}} = 3.2177, \overline{\frac{AND_{CUSUM}}{AND_{np\text{-}CUSUM}}} = 1.0504 \text{ and } \overline{\frac{AND_{EWMA}}{AND_{np\text{-}CUSUM}}} = 1.1102.$$

This indicates that, from the most comprehensive viewpoint (covering all different values of τ, p_0, p_{max} and n), the np-CUSUM scheme is more effective than the np chart, CUSUM chart and EWMA chart by 221.77%, 5.04% and 11.02%, respectively.

It is noteworthy that neither the np chart nor the CUSUM chart can have higher overall effectiveness than the np-CUSUM scheme under any circumstances (for any set of specifications τ, p_0, p_{max} and n), because each of the np chart and CUSUM chart is just a special case of the np-CUSUM scheme. If the control limit H of an np-CUSUM scheme is set infinitely large and its *UCL* is made equal to that of an np chart, then this np-CUSUM scheme will perform exactly as that np chart. Similarly, if the upper limit *UCL* of the np-CUSUM scheme is set infinitely large and its *H* and *k* are made equal to those of a CUSUM chart, then the np-CUSUM scheme works exactly as the CUSUM chart. Consequently, one can always design an np-CUSUM scheme that will surely perform better than, or at least equally well as, the best np chart or the best CUSUM chart. As shown in Table 2, there is one special case (case 5) in which the np-CUSUM scheme and CUSUM chart are equivalent and both produce the same results. In all other cases, the np-CUSUM scheme outperforms both the np chart and CUSUM chart.

Finally, the performance of the np-CUSUM scheme is compared with that of the M-P np-CUSUM chart proposed by Morais and Pacheco (2006) under the following specifications used in one example in their paper:

$$\tau = 240,\ p_0 = 0.05 \text{ and } n = 100 \tag{12}$$

Since Morais and Pacheco (2006) have not specified a value for the maximum fraction non-conforming $p_{\max}$, a setting of ($p_{\max} = 10p_0$) is used for this study. The charting parameters of the M-P np-CUSUM chart as determined by Morais and Pacheco (2006) are $k = 5.29$, $H = 18.3$ and $UCL = 8.79$. However, these parameters values will produce a very small ATS_0 of 15 which seriously violates the constraint ($ATS_0 \geq \tau$). In order to ensure a fair and meaningful comparison between the charts, the *UCL* of the M-P np-CUSUM chart has been relaxed from 8.79 to 15 so that ATS_0 approaches the value of τ (= 240) as specified by Morais and Pacheco (2006). In addition, the CUSUM chart and np-CUSUM scheme are also designed for this case. The three charts are shown below:

M-p np-CUSUM chart: $k = 5.290,\ H = 18.300,\ UCL = 15,\ AND = 0.193$

CUSUM chart: $k = 9.750,\ H = 2.406,\ AND = 0.186$

np-CUSUM scheme: $k = 7.250,\ H = 4.971,\ UCL = 15,\ AND = 0.172.$

The ratios of $AND_{M\text{-}P\ np\text{-}CUSUM}/AND_{CUSUM}$ and $AND_{M\text{-}P\ np\text{-}CUSUM}/AND_{np\text{-}CUSUM}$ are 1.038 and 1.122, respectively. This indicates that, The CUSUM chart and np-CUSUM scheme reduce the *AND* by about 4% and 12%, respectively, compared with the M-P np-CUSUM chart. The fact that the M-P np-CUSUM chart is even inferior to the single CUSUM chart reflects that simply combining an np chart and a CUSUM chart together without optimising the charting parameters may not ensure better performance.

4 Case study

This case study concerns the quality of a surgical sponge product. A control chart is to be designed to monitor the fraction non-conforming of the product. The in-control p_0 is estimated as 0.0125 from historical records. Based on the requirement on quality and the experience of the quality engineer on the process, the maximum fraction non-conforming $p_{\max}$ is set as $10p_0$. The allowable minimum τ is set as 700 hours. A sample size n of 80 and a sampling interval h of 1 hour is selected based on the available manpower and working shift. The specifications are summarised as follows:

$p_0 = 0.0125$,	in-control fraction non-conforming
$p_{\max} = 10\,p_0$,	maximum fraction non-conforming
$\tau = 700$ hours,	allowance minimum in-control ATS_0
$n = 80$,	sample size
$h = 1$ hour,	sampling interval.

The charting parameters of the np chart, CUSUM chart and np-CUSUM scheme as well as their *AND* and $AND/AND_{np\text{-}CUSUM}$ values are listed below:

np chart:	$UCL = 5$, $AND = 0.312$, $AND/AND_{np\text{-}CUSUM} = 2.737$
CUSUM chart:	$k = 1.500$, $H = 6.006$, $AND = 0.125$, $AND/AND_{np\text{-}CUSUM} = 1.096$
np-CUSUM scheme:	$k = 1.750$, $H = 4.779$, $UCL = 5$, $AND = 0.114$.

Table 3 Comparison of the three charts in the case study

$p(\times p_0)$	*ATS*		
	np chart	*CUSUM chart*	*np-CUSUM chart*
1	1,922.5508	919.1721	765.1227
2	65.2263	11.3406	13.4938
3	11.9924	4.0386	4.0107
4	4.2444	2.5171	2.1970
5	2.1044	1.7522	1.4574
6	1.2838	1.3618	1.0567
7	0.9065	1.1006	0.8233
8	0.7150	0.9163	0.6849
9	0.6132	0.7775	0.6017
10	0.5585	0.6769	0.5541

Figure 2 *ATS* of the three control charts in the case study

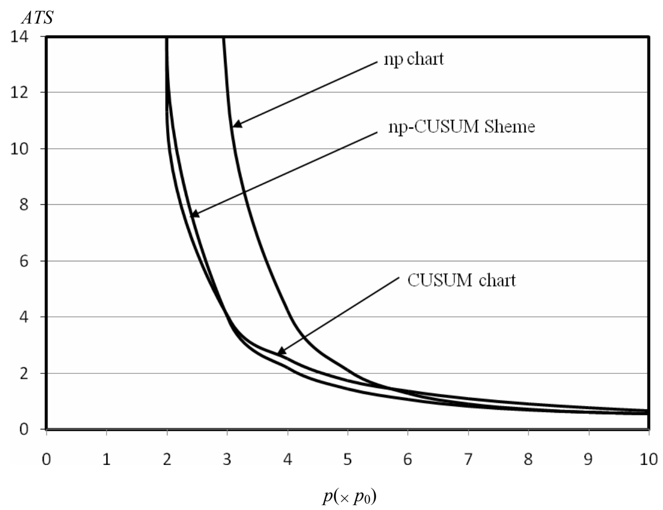

(a)

Figure 2 *ATS* of the three control charts in the case study (continued)

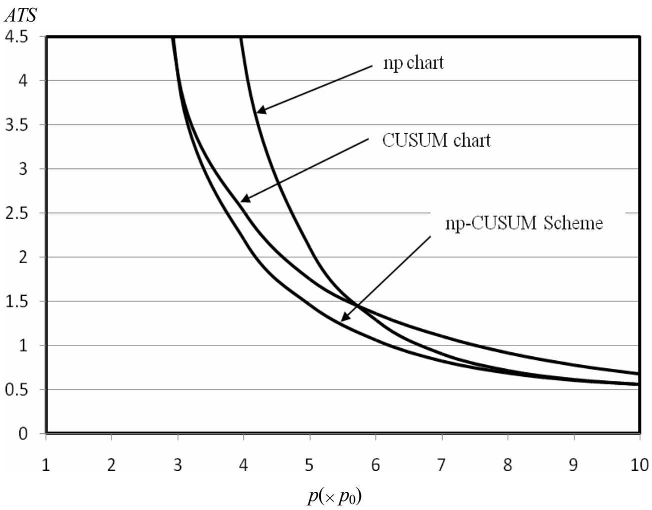

(b)

In this case study, in terms of *AND* values, the np-CUSUM scheme reduces the *AND* by about 174% and 10% compared with the np chart and CUSUM chart, respectively. The values of the in-control ATS_0 (where $p = p_0$) and out-of-control *ATS* (where $p_0 < p \leq 10p_0$) of the three charts are shown in Table 3. The curves of the *ATS* value versus *p* of the three charts are illustrated in Figure 2. Figure 2(a) shows the *ATS* curves over nearly the whole shift range while Figure 2(b) zooms in the *ATS* curves under moderate and large *p* shifts. It can be observed that the np-CUSUM scheme outperforms the np chart over the entire *p* shift range. The np-CUSUM scheme is also more effective than the CUSUM chart over the whole *p* shift range except for $p = 2p_0$.

5 Discussions and conclusions

This article presents an algorithm for the optimisation design of the np-CUSUM scheme which comprises an np chart element and a CUSUM chart element. The design algorithm does not only optimise the charting parameters of each of the np chart element and CUSUM chart element, but also optimises the allocation of the detection power between the two elements, so that the best overall performance can be achieved.

Moreover, systematic performance assessment and comparison have been carried out. The results of the comparative studies show that the optimisation design makes the np-CUSUM scheme always outperform, or at least perform equally as, the np chart, CUSUM chart and EWMA chart in terms of *AND*. The np-CUSUM scheme is more effective than the main competitor, the CUSUM chart, by 5% on average in terms of *AND*.

As a by-product of the optimisation design, the resultant ATS_0 of the np-CUSUM scheme is usually close to the specification τ in spite of the discrete nature of the attribute quality characteristics. This feature enables the designers of the np-CUSUM scheme to accurately specify and control the false alarm rate and, at the same time, to make full use of the potential of the detection effectiveness of the chart.

Due to the rapid advancement in computational technology, the complexity of the implementation of the np-CUSUM scheme is almost the same as that of the np chart, CUSUM chart and EWMA chart. Since the np-CUSUM scheme considerably outperforms the other charts, it is recommended that the individual charts be replaced by the np-CUSUM scheme for attribute SPC. The whole optimisation design of the np-CUSUM scheme can be implemented with a computer programme by following a well developed procedure. Once the optimisation design is carried out, the designed np-CUSUM scheme can be used continuously and the improvement in detection effectiveness can be benefited on a long term basis.

In this article, the studies are conducted based on some general conventions and assumptions, such as the known in-control fraction non-conforming p_0 and the binomial distribution of d. It is interesting to carry out further studies on how the performance of the np-CUSUM scheme will be affected when p_0 is estimated and d follows other distributions.

In this article, both the sample size n and sampling interval h are specified or fixed for each design case with n depending on the available inspection resource and h following the rational subgroup concept. However, in some applications, n and h are allowed to be adjusted under some constraints on inspection rate or cost. Therefore, it is also worthwhile, as a future work, to search the optimal values of n and h of an np-CUSUM scheme for such applications.

Another promising future research is to investigate an adaptive np-CUSUM chart in which the sample size n and sampling interval h are varied based on the online observed data from the process (Wu and Luo, 2004). The adaptive np-CUSUM chart is expected to detect process changes even faster than its static counterpart with fixed n and h, as well as the adaptive np and CUSUM charts. However, the design and implementation of the adaptive charts are more complicated. The operational difficulty cannot be simply solved by just using an on-site computer.

Acknowledgements

The authors would like to thank the referees for constructive comments that greatly improved the presentation of this paper.

References

Abel, V. (1990) 'On one-sided combined Shewhart-CUSUM quality control schemes for Poisson counts', *Computational Statistics Quarterly*, Vol. 6, pp.31–39.

Bourke, P.D. (2001) 'Sample size and the binomial CUSUM control chart: the case of 100% inspection', *Metrika*, Vol. 53, No. 1, pp.51–70.

British Standard Institution (1985) *Quality Management Systems, BSI Handbook 24*, Quality Control, London.

Brook, D. and Evans, D.A. (1972) 'An approach to the probability distribution of CUSUM run length', *Biometrika*, Vol. 59, No. 3, pp.539–549.

Chan, K.Y., Chan, K.W., Pong, G.T.Y., Aydin, M.E., Fogarty, T.C. and Ling, S.H. (2009) 'A statistics-based genetic algorithm for quality improvements of power supplies', *European Journal of Industrial Engineering*, Vol. 3, No. 4, pp.468–492.

Epprecht, E.K., Simões, B.F. and Mendes, F.C. (2010) 'A variable sampling interval EWMA chart for attributes', *International Journal of Advanced Manufacturing Technology*, Vol. 49, Nos. 1–4, pp.281–292.

Gan, F.F. (1993) 'An optimal design of CUSUM control charts for binomial counts', *Journal of Applied Statistics*, Vol. 20, No. 4, pp.445–460.

Garcia-Diaz, J.C. (2007) 'The 'effective variance' control chart for monitoring the dispersion process with missing data', *European Journal of Industrial Engineering*, Vol. 1, No. 1, pp.40–55.

Hawkins, D.M. (1992) 'Evaluation of average run lengths of cumulative sum charts for an arbitrary data distribution', *Communications in Statistics-Simulation and Computation*, Vol. 21, No. 4, pp.1001–1020.

Lucas, J.M. (1982) 'Combined Shewhart-CUSUM quality control schemes', *Journal of Quality Technology*, Vol. 14, No. 2, pp.51–59.

Lucas, J.M. (1985a) 'Counted data CUSUM's', *Technometrics*, Vol. 27, No. 2, pp.129–144.

Lucas, J.M. (1985b) 'Cumulative sum (CUSUM) control schemes', *Communications in Statistics-Theory and Methods*, Vol. 14, No. 11, pp.2689–2704.

Lucas, J.M. (1989) 'Control schemes for low count levels', *Journal of Quality Technology*, Vol. 21, No. 3, pp.199–201.

Montgomery, D.C. (2009) *Introduction to Statistical Quality Control*, 6th ed., John Wiley & Sons, New York.

Morais, M. and Pacheco, A. (2006) 'Combined CUSUM-Shewhart schemes for binomial data', *Economic Quality Control*, Vol. 1, No. 1, pp.43–57.

Nelson, L.S. (1988) 'Control charts: rational subgroups and effective applications', *Quality Technology*, Vol. 20, No. 1, pp.73–75.

Parveen, M. and Rao, T.V. (2009) 'Optimal batch sizing, quality improvement and rework for an imperfect production system with inspection and restoration', *European Journal of Industrial Engineering*, Vol. 3, No. 3, pp.305–335.

Radaelli, G. (1994) 'Poisson and negative binomial dynamics for counted data under CUSUM-type charts', *Journal of Applied Statistics*, Vol. 21, No. 5, pp.347–356.

Raj, T. and Attri, R. (2010) 'Quantifying barriers to implementing total quality management (TQM)', *European Journal of Industrial Engineering*, Vol. 4, No. 3, pp.308–335.

Reynolds, M.R. Jr., Amin, R.W. and Arnold, J.C. (1990) 'CUSUM charts with variable sampling intervals', *Technometrics*, Vol. 32, No. 4, pp.371–384.

Reynolds, M.R. Jr. and Stoumbos, Z.G. (1999) 'A CUSUM chart for monitoring a proportion when inspecting continuously', *Journal of Quality Technology*, Vol. 31, No. 1, pp.87–108.

Reynolds, M.R. Jr. and Stoumbos, Z.G. (2000) 'A general approach to modeling CUSUM charts for a proportion', *IIE Transaction*, Vol. 32, No. 6, pp.515–535.

Reynolds, M.R. Jr. and Stoumbos, Z.G. (2004a) 'Control charts and the efficient allocation of sampling resources', *Technometrics*, Vol. 46, No. 2, pp.200–214.

Reynolds, M.R. Jr. and Stoumbos, Z.G. (2004b) 'Should observations be grounded for effective process monitoring', *Journal of Quality Technology*, Vol. 36, No. 4, pp.343–366.

Roberts, S.W. (1959) 'Control chart tests based on geometric moving averages', *Technometrics*, Vol. 1, No. 3, pp.239–250.

Shu, L., Jiang, W. and Tsui, K.L. (2008) 'A weighted CUSUM chart for detecting patterned means shifts', *Journal of Quality Technology*, Vol. 40, No. 2, pp.194–213.

White, C.L. and Keats, J.B. (1996) 'ARLs and higher-order run-length moments for the Poisson CUSUM', *Journal of Quality Technology*, Vol. 28, No. 3, pp.363–369.

White, C.L., Keats, J.B. and Stanley, J. (1997) 'Poisson CUSUM vs. c chart for defect data', *Quality Engineering*, Vol. 9, No. 4, pp.673–679.

Woodall, W.H. (1984) 'On the Markov chain approach to the two-sided CUSUM procedures', *Technometrics*, Vol. 26, No. 1, pp.41–46.

Woodall, W.H. and Montgomery, D.C. (1999) 'Research issues and ideas in statistical process control', *Journal of Quality Technology*, Vol. 31, No. 4, pp.376–386.

Wu, Z., Jiao, J. and Liu, Y. (2008a) 'A binomial CUSUM chart for detecting large shifts in fraction nonconforming', *Journal of Applied Statistics*, Vol. 35, No. 11, pp.1267–1276.

Wu, Z. and Luo, H. (2004) 'Optimal design of the adaptive sample size and sample interval np control chart', *Quality and Reliability Engineering International*, Vol. 20, No. 6, pp.553–570.

Wu, Z., Luo, H. and Zhang, X.L. (2006) 'Optimal np control chart with curtailment', *European Journal of Operational Research*, Vol. 174, No. 3, pp.1723–1741.

Wu, Z. and Tian, Y. (2005) 'Weighted-loss-function CUSUM chart for monitoring mean and variance of a production process', *International Journal of Production Research*, Vol. 43, No. 14, pp.3027–3044.

Wu, Z., Yang, M., Jiang, W. and Khoo, M.B. (2008b) 'Optimization designs of the combined Shewhart-CUSUM control charts', *Computational Statistics & Data Analysis*, Vol. 53, No. 2, pp.496–506.

Yashchin, E. (1985) 'On the analysis and design of CUSUM-Shewhart control schemes', *IBM Journal of Research and Development*, Vol. 29, No. 4, pp.377–391.

Zhao, Y., Tsung, F. and Wang, Z.J. (2005) 'Dual CUSUM control scheme for detecting a range of mean shift', *IIE Transactions*, Vol. 37, No. 11, pp.1047–1058.

Appendix

Calculation of the in-control ATS_0 and out-of-control ATS for the np-CUSUM scheme

The cumulative probability function $F_d(D)$ of d can be calculated as follows:

$$F_d(D) = \Pr(d \le D) = \sum_{i=0}^{D} C_i^n p^i (1-p)^{n-i}, \qquad C_i^n = \frac{n!}{i!(n-i)!} \tag{A1}$$

The np-CUSUM scheme is a combined scheme of a CUSUM chart element with parameters (H and k) and an np chart element with parameter (UCL). The np-CUSUM scheme can be described by a Markov chain procedure. Suppose that the statistic C_t in equation (2) experiences M different transitional states before being absorbed into the out-of-control state. States 0 to (M – 1) are the in-control states and state M is an out-of-control state. The width Δ of the interval of each state is given by:

$$\Delta = H / (M - 0.5), \tag{A2}$$

The centre, O_i, of state i is given by:

$$O_i = i \cdot \Delta \qquad i = 0, 1, \ldots, M. \tag{A3}$$

The transition probability p_{ij} from state i to state j of the np-CUSUM scheme is determined as follows:

for $j = 0$,

$$p_{i0} = \begin{cases} F_d[(0.5-i)\Delta + k] & \text{if} \quad UCL > (0.5-i)\Delta + k \\ F_d[UCL] & \text{if} \quad UCL < (0.5-i)\Delta + k \end{cases} \tag{A4}$$

for $j > 0$,

$$p_{ij} = \begin{cases} F_d[u] - F_d[l] & \text{if} \quad UCL > u \\ F_d[UCL] - F_d[l] & \text{if} \quad l < UCL < u \\ 0 & \text{if} \quad UCL < l \end{cases} \tag{A5}$$

where $l = (j - i - 0.5)\Delta + k$ and $u = l + \Delta$

When evaluating the in-control ARL_0, p_{ij} is calculated using $p = p_0$. Based on p_{ij}, the in-control transition probability matrix $\boldsymbol{R_0}$ is established. It is a $M \times M$ matrix excluding the elements associated with the absorbing (i.e., out-of-control) state.

$$\boldsymbol{R_0} = \begin{bmatrix} p_{00} & p_{01} & \cdots & p_{0,M-1} \\ p_{10} & p_{11} & \cdots & p_{1,M-1} \\ \vdots & \vdots & \vdots & \vdots \\ p_{M-1,0} & p_{M-1,1} & \cdots & p_{M-1,M-1} \end{bmatrix} \tag{A6}$$

ARL_0 is equal to the first element of vector $\boldsymbol{U}$ given by the following expression:

$$\boldsymbol{U} = \left(\boldsymbol{I} - \boldsymbol{R_0}\right)^{-1} \mathbf{1}, \tag{A7}$$

where $\boldsymbol{I}$ is an identity matrix and $\mathbf{1}$ is a vector with all elements equal to one. Finally, ATS_0 can be calculated from ARL_0.

$$ATS_0 = ARL_0 \cdot h. \tag{A8}$$

The transition probability matrix $\boldsymbol{R_1}$ for calculating the out-of-control ARL can be established similarly as $\boldsymbol{R_0}$ except that the transition probability p_{ij} of $\boldsymbol{R_1}$ must be evaluated according to the out-of-control p. It is assumed that the statistic C_t has reached its stationary distribution at the time when the p shift occurs and that the random time of process shift has a uniform distribution within the sampling interval (Reynolds et al., 1990). Based on these assumptions, the steady-state ARL is calculated below:

$$ARL = \boldsymbol{B}^T \left[\left(\boldsymbol{I} - \boldsymbol{R_1}\right)^{-1} \mathbf{1} - \mathbf{1}/2\right], \tag{A9}$$

where $\boldsymbol{B}$ is the steady-state probability vector under ($p = p_0$). It is obtained by first normalising the matrix $\boldsymbol{R_0}$ (making the sum of the elements in each row equal to one), and then solving the following equation:

$$\boldsymbol{B} = \boldsymbol{R}_0^T \boldsymbol{B}, \tag{A10}$$

subjected to

$$\mathbf{1}^T \boldsymbol{B} = 1. \tag{A11}$$

At last, *ATS* can be calculated from *ARL*.

$$ATS = ARL \cdot h. \tag{A12}$$

All of the formulae derived in the Appendix have been checked by simulation.